

UCSF

UC San Francisco Previously Published Works

Title

Semimechanistic models to relate noxious stimulation, movement, and pupillary dilation responses in the presence of opioids

Permalink

<https://escholarship.org/uc/item/8vd3q9zj>

Journal

CPT Pharmacometrics & Systems Pharmacology, 11(5)

ISSN

2163-8306

Authors

Marco-Ariño, Nicolás
Vide, Sergio
Agustí, Mercè
et al.

Publication Date

2022-05-01

DOI

10.1002/psp4.12729

Peer reviewed

ARTICLE

Semimechanistic models to relate noxious stimulation, movement, and pupillary dilation responses in the presence of opioids

Nicolás Marco-Ariño^{1,2} | Sergio Vide^{3,4} | Mercè Agustí³ | Andrew Chen³ |
 Sebastián Jaramillo³ | Itziar Irurzun-Arana^{1,2} | Adrià Pacheco³ | Carmen Gonzalez⁵ |
 Erik W. Jensen⁵ | Patricia Capsi-Morales³ | José F. Valencia^{3,6} | Iñaki F. Troconiz^{1,2} |
 Pedro L. Gambus^{3,7} | Merlin D. Larson^{3,8}

¹Pharmacometrics & Systems Pharmacology, Department of Pharmaceutical Technology and Chemistry, School of Pharmacy and Nutrition, University of Navarra, Pamplona, Spain

²Instituto de Investigación Sanitaria de Navarra, Pamplona, Spain

³Systems Pharmacology Effect Control & Modeling Research Group, Anesthesiology Department, Hospital Clinic de Barcelona, Barcelona, Spain

⁴Center for Clinical Research in Anesthesia, Serviço de Anestesiologia, Centro Hospitalar do Porto, Porto, Portugal

⁵Department of Research and Development, Quantum Medical, Mataró, Barcelona, Spain

⁶Electronic Engineering Program, School of Engineering, Universidad de San Buenaventura, Cali, Colombia

⁷Neuroimmunology Research Group, Institut d'Investigacions Biomèdiques August Pi I Sunyer, Barcelona, Spain

⁸Department of Anesthesia and Perioperative Care, University of California San Francisco, San Francisco, California, USA

Abstract

Intraoperative targeting of the analgesic effect still lacks an optimal solution. Opioids are currently the main drug used to achieve antinociception, and although underdosing can lead to an increased stress response, overdose can also lead to undesirable adverse effects. To better understand how to achieve the optimal analgesic effect of opioids, we studied the influence of remifentanyl on the pupillary reflex dilation (PRD) and its relationship with the reflex movement response to a standardized noxious stimulus. The main objective was to generate population pharmacodynamic models relating remifentanyl predicted concentrations to movement and to pupillary dilation during general anesthesia. A total of 78 patients undergoing gynecological surgery under general anesthesia were recruited for the study. PRD and movement response to a tetanic stimulus were measured multiple times before and after surgery. We used nonlinear mixed effects modeling to generate a population pharmacodynamic model to describe both the time profiles of PRD and movement responses to noxious stimulation. Our model demonstrated that movement and PRD are equally depressed by remifentanyl. Using the developed model, we changed the intensity of stimulation and simulated remifentanyl predicted concentrations maximizing the probability of absence of movement response. An estimated effect site concentration of 2 ng/ml of remifentanyl was found to inhibit movement to a tetanic stimulation with a probability of 81%.

Study Highlights

WHAT IS THE CURRENT KNOWLEDGE ON THE TOPIC?

Movement is a known response to noxious stimulus. However, its applicability to assess intraoperative nociception is limited when neuromuscular blocking agents

Iñaki F. Troconiz, Pedro L. Gambus, and Merlin D. Larson supervised the project and share senior authorship of this article.

This is an open access article under the terms of the [Creative Commons Attribution-NonCommercial-NoDerivs](https://creativecommons.org/licenses/by-nc-nd/4.0/) License, which permits use and distribution in any medium, provided the original work is properly cited, the use is non-commercial and no modifications or adaptations are made.

© 2021 The Authors. *CPT: Pharmacometrics & Systems Pharmacology* published by Wiley Periodicals LLC on behalf of American Society for Clinical Pharmacology and Therapeutics.

Correspondence

Pedro L. Gambus, Department of Anesthesiology, Hospital CLINIC de Barcelona, Carrer de Villarroel 170, 08036, Barcelona, Spain.
Email: plgambus@ub.edu

Funding

Not applicable.

are used. Pupillary reflex dilation (PRD) is known to predict movement after noxious stimuli and to be useful in assessing nociception response.

WHAT QUESTION DID THIS STUDY ADDRESS?

This study aimed to quantitatively relate PRD and movement with noxious stimulation and opioids to gain an understanding of the underlying mechanisms that control both variables.

WHAT DOES THIS STUDY ADD TO OUR KNOWLEDGE?

This study provides a granular description of PRD and movement reflex to tetanic stimulation, which were characterized with semimechanistic population pharmacodynamic models. PRD and movement showed similar responses to painful stimulation and remifentanyl, supporting the hypothesis that both reflexes share a common physiological mechanism of control.

HOW MIGHT THIS CHANGE DRUG DISCOVERY, DEVELOPMENT, AND/OR THERAPEUTICS?

This study provides evidence for the use of PRD as a surrogate marker for pain, guiding opioid administration during surgery.

INTRODUCTION

Titration of opioids during surgery must be performed according to the intensity of external stimuli to attain the right nociceptive–antinociceptive balance. The estimation of this balance depends on reflex quantification of responses to stimulation and nonspecific autonomic responses as well as previous clinical experience. The most direct and clinically observed reflex response to noxious stimulation is movement. Other indirect signs derived from the autonomic nervous system stimulation such as arterial hypertension, tachycardia, sweating, or presence of tears have also been clinically used as surrogate measures of response to noxious stimulation.¹ These indirect signs can be affected by changes that are not related to painful stimulation. Therefore, the pursuit for the individualization of the analgesic component of general anesthesia^{2,3} lead to the development and commercialization of different nociception indexes/monitors. One such monitor quantitates pupillary reflex dilation (PRD) to a homogenous electrical painful stimulation. PRD is a supra-spinal parasympathetic reflex present during general anesthesia^{4,5} shown to be triggered by noxious stimuli in anesthetized subjects.^{6,7} This reflex is diminished by opioid administration,⁸ suggesting it could be used for the assessment of analgesia in patients under general anesthesia.

Reflex movement to a noxious stimulus is considered to be a classical response, and its generation involves the transmission of nociceptive signals from the periphery to the central nervous system and includes the modulation by the rostral ventral medulla (RVM), where “on-cells” and “off-cells” are present. In the close vicinity of these areas, the control mechanisms of the PRD are located. Some authors have shown that the effect of externally

administered opioids can affect the normal function of “off-cells,” preventing the noxious stimuli to progress toward the cortex and hence blocking any movement response.^{9,10} Similarly, the presence of opioids prevents the dilation mechanism of the pupil from working.¹¹

To better understand the effects of opioids on PRD and its relationship with the reflex movement response to nociception, we conducted a prospective clinical study where patients under the effects of propofol received varying target concentrations of the opioid remifentanyl to observe and quantitate the movement and PRD responses elicited by a homogenous painful electrical stimulation. The main objective was to generate a population model relating remifentanyl concentration to movement and to pupillary dilation. Based on the developed model, we simulated possible opioid dosing schemes, maximizing the probability of the absence of movement response, that is, cortical repercussion of pain, in unconscious patients under general anesthesia.

METHODS

Patient population and characteristics

Under Institutional Review Board and Ethics Committee approval (Hospital Clinic de Barcelona no. HCB/2016/0318) and following written informed consent, 78 female patients scheduled for gynecologic surgery under general anesthesia in the Ambulatory Surgery facility at Hospital Clinic de Barcelona, Spain, were included in the current study. Exclusion criteria were prior eye surgery, any ophthalmologic diseases besides refraction errors, prescription of drugs affecting the size or reflex of the pupil, and morbid obesity (body mass index > 35).

Study protocol

Upon arrival in the operating room, routine monitors were placed. General anesthesia was achieved and maintained with propofol and remifentanyl administered using a Target-Controlled Infusion system (Base Primea, Fresenius Kabi AG, Bad Homburg, Germany).

Loss of consciousness was induced setting the effect site concentration of propofol ($C_{e,prop}$) between 5 and 11 $\mu\text{g}/\text{ml}$ (Schnider et al.^{12,13}).

PRD measurements and reflex movement assessment

Two minutes after reaching the predicted pseudo-steady state for propofol, the PRD was elicited using the videopupillometer Algiscan® (IDMed, Marseille, France) connected to two electrodes placed on the volar surface of the right arm. The stimulus consisted of a 60 mA tetanus for a period of 5 s. Pupillary diameter (PDiam) was measured and recorded at 67 Hz for 13 s: 2 s before the stimulation, during the 5 s stimulation, and until 6 s after the stimulation ended. A rubber cup covered the measured eye, and the contralateral eye was taped closed.

The investigational procedure was video recorded. Retrospectively, two clinicians examined the video recordings to evaluate intensity and duration of the movement response. Movement intensity was classified into the following four-level categorical scale: 0 = absence of movement, 1 = movement of only one limb, 2 = movement of two or three limbs, and 3 = movement of the whole body.

Within approximately 5 min after the first stimulation, while maintaining the same propofol effect site concentration, remifentanyl administration was started, achieving predicted effect site concentrations ($C_{e,remi}$)¹⁴ varying between 0.5 and 6 ng/ml. Two minutes after reaching the predicted pseudo-steady state equilibration, a second and a third PRDs were elicited as described previously, and PDiam and movement response were recorded.

Then airway was then secured either by placement of a laryngeal mask or by endotracheal intubation. When intubation was required, 30 mg of rocuronium bromide were administered, two minutes before laryngoscopy. The hypnotic effect was titrated to maintain a Bispectral Index (BIS Vista, Medtronic, Ireland) value between 45 and 60. The analgesic effect was titrated at the discretion of the attending anesthesiologist.

At the end of surgery $C_{e,prop}$ and $C_{e,remi}$ were set to 1 $\mu\text{g}/\text{ml}$ and 0 ng/ml, respectively. When the propofol C_e target was reached, one or two additional stimulations separated by at least 3 min were carried out before the patient spontaneously awakened or moved.

General description of the data

Figure 1 shows the raw data profiles for pupillary size, movement response, and drug concentrations used for the model development. Of all pupil measurements, 1082 were recorded in the presence of propofol (first stimulus), and 2775 were recorded with a combination of propofol and remifentanyl (stimuli 2–4). For the movement analysis, 1092 observations correspond to the first stimulus and 2816 to stimuli 2–4. In both end points, the number of observations after surgery was lower than for those performed before surgery started as patients were recovering consciousness after the surgical procedure, and measures were interrupted when patients showed signs of arousal. Predicted propofol and remifentanyl concentrations were recorded every second during the experimental procedure.

Data analysis

PRD and movement data were fit separately. All of the analyses were carried out using the population approach with nonlinear mixed effects modeling and the software NONMEM 7.4.¹⁵ The first-order conditional estimation method with interaction was used for the analysis of the PDiam (continuous data). The movement response was treated as an ordered categorical variable and analyzed using the Laplacian estimation method instead.

Interindividual variability (IIV) was modeled exponentially for parameters integrating the model of the PDiam. On the other hand, an additive model was used to describe IIV associated with the Logit (L) analysis of movement scores because regardless of the magnitude of the individual random effect, probabilities were kept between 0 and 1. PDiam data were logarithmically transformed for the analysis, and the residual error was modeled initially with an additive model in the logarithmic scale. Given the fact that PDiam were measured very frequently, autocorrelation should not be ruled out, and a model for autocorrelated errors¹⁶ was also explored in the analysis as indicated by an anonymous reviewer. Residual variability does not apply in the case of the analysis of noncontinuous response.

Pharmacodynamic models

The raw data profiles presented in Figure 1 show two features that are relevant from a modeling point of view: (i) there is a delay between the beginning of the nociceptive electric impulse and the onset of the pupil and movement responses, and (ii) remifentanyl reduces both the PDiam and the probability of movement. Consequently, models

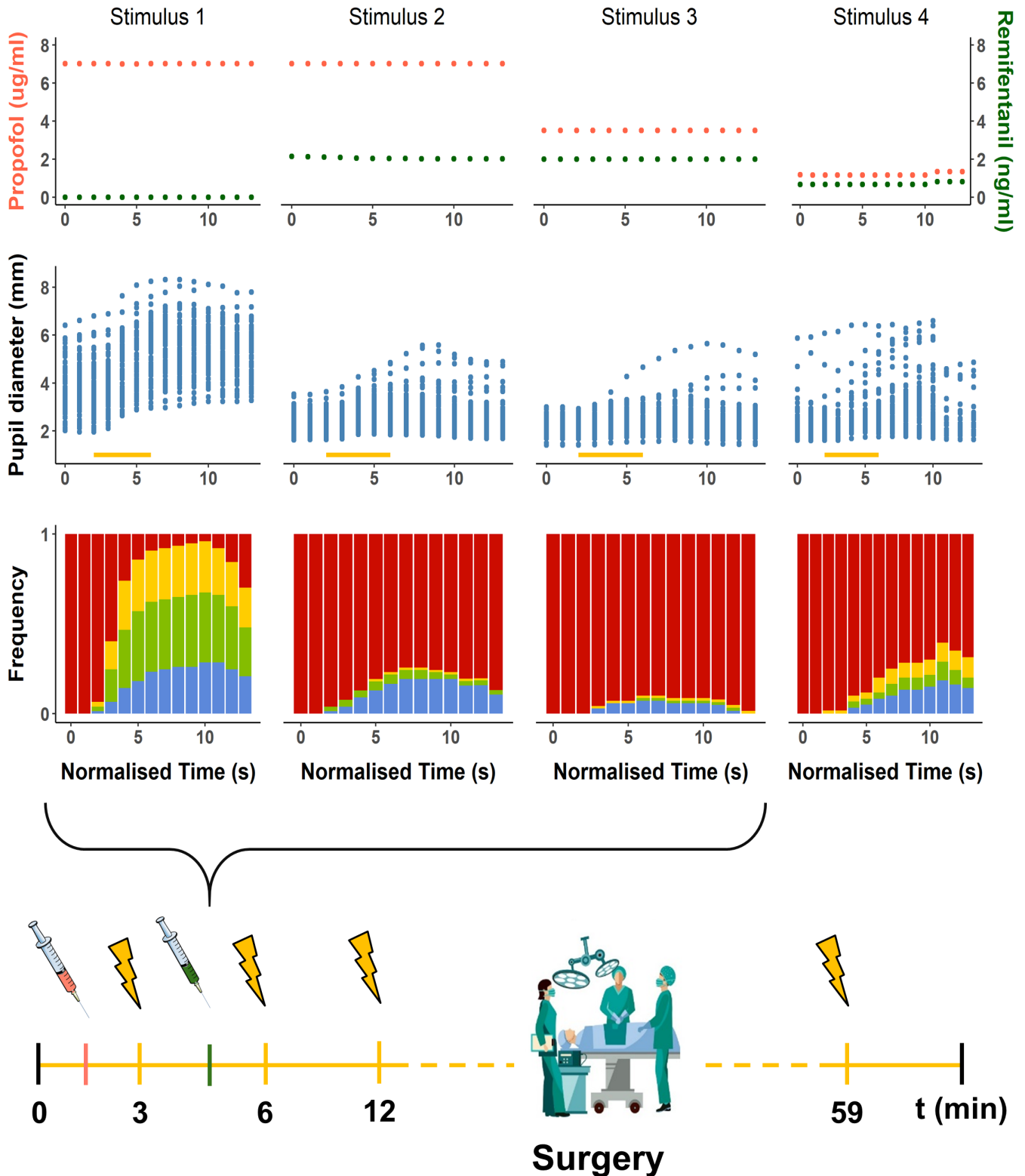


FIGURE 1 Overview of the experimental set-up and data generated during the experimental procedure. Upper panels show the median concentrations of propofol (red) and remifentanyl (green) over the four cycles of stimulation. Middle panels depict the raw pupil profiles for each stimulus. Orange line highlights the period of 5 s when electric stimulation is delivered. Lower panels represent the distribution of the movement scores per stimulus (Grade 0, red; Grade 1, blue; Grade 2, green; Grade 3, yellow). The bottom figure represents the timeline of the experimental procedure with the administration of propofol (red syringe), electric stimuli (yellow lightning), administration of remifentanyl (green syringe), and surgical procedure. Times represent the mean starting time for each stimulus among all the individuals. Images were modified from Servier Medical Art⁴⁷ and Freepik⁴⁸

based on the concept of the indirect response,¹⁷ and drug inhibitory effects either on the perception and/or transduction of the nociceptive signal, were fit to the data.

Models assume that the degree of activation of unobserved levels of nociceptors (N_{act}) drive the pupil and movement response. In absence of either electric stimulation or remifentanyl, N_{act} was arbitrarily set to a baseline value of 1 ($N_{act,0}$), maintained by the balance between the zero and first-order rate constants of turnover, K_S and K_D , respectively, as shown by Equation (1). At baseline, the rate of change of N_{act} (dN_{act}/dt) is null, and K_S equal K_D as $N_{act,0} = 1$.

$$\frac{dN_{act}}{dt} = K_S - K_D \times N_{act,0} \quad (1)$$

Electric stimulation increases N_{act} as indicated in Equation (2), where θ_{ES} is the parameter accounting for its nociceptive effects, and ES is a variable with a value of 1 during the application of the electrical stimulus and 0 otherwise.

Analgesic effects of remifentanyl were explored as a modulation of θ_{ES} , and/or increasing K_D , the first-order rate constant of nociceptor deactivation, and are expressed in Equation (2) by $f(C_{e,remi})$, and $g(C_{e,remi})$, respectively.

$$\frac{dN_{act}}{dt} = K_S \times [1 + \theta_{ES} \times ES \times f(C_{e,remi})] - K_D \times g(C_{e,remi}) \times N_{act} \quad (2)$$

During model development, different structures for $f()$ and $g()$ considering the predicted remifentanyl concentration in plasma ($C_{p,remi}$) and effect site ($C_{e,remi}$) were explored as shown in the Results section. Predicted values of $C_{e,remi}$ were obtained using Equation (3) representing the effect compartment model.¹⁷ Contribution of propofol to the activation of nociceptors was also investigated.

$$\frac{dC_{e,remi}}{dt} = k_{e0} \times (C_{p,remi} - C_{e,remi}) \quad (3)$$

where k_{e0} , is the first-order rate constant governing the drug distribution equilibrium between the central and effect site compartments.

PRD response

A turnover model was used to transduce the N_{act} dynamics to PRD as shown in Equation (4), where $K_{P,S}$ and $K_{P,D}$ represent the zero-order and first-order rate turnover constants, respectively, being $K_{P,S} = K_{P,D} \times PDiam_0$, and $PDiam_0$, the value of $PDiam$ at baseline.

$$\frac{dPDiam}{dt} = K_{P,S} \times N_{act} - K_{P,D} \times PDiam \quad (4)$$

Additional effects of remifentanyl on the turnover parameters were explored, in addition to the possibility that differences in $PDiam$ and N_{act} dynamics were negligible. The contribution of propofol to the activation of nociceptors and pupil turnover was also investigated. Linear and nonlinear inhibitory models as well as an effect site compartment were evaluated.

Reflex movement response

Movement response was recorded as an ordered categorical variable and was modeled using the proportional odds logistic regression approach. The cumulative conditional probability of observing a score greater than or equal to a certain m category in the i th subject at the j th observation time is denoted $P(Y_{ij} \geq m|\eta_i)$ and is described by Equation (5), where η_i is the individual random effect that belongs to a distribution of mean 0 and variance ω^2 .

$$P(Y_{ij} \geq m|\eta_i) = \frac{e^L}{1 + e^L} \quad (5)$$

L , the logit, brings together the parameters defining the baseline probabilities of movement, and the contribution of N_{act} represented in Equation (6) as θ_k and $h(N_{act})$, respectively.

$$L = \sum_{k=1}^m \theta_k + h(N_{act}) + \eta_i \quad (6)$$

Finally, the probability of observing an m score $P(Y_{ij} = m|\eta_i)$ is given by the following expression (Equation 7):

$$P(Y_{ij} = m|h_i) = P(Y_{ij} \geq (m - 1) |h_i) - P(Y_{ij} \geq m|h_i) \quad (7)$$

The contribution of first-order Markov elements to the movement response was explored as well as considering the nonproportional odds approach and the inclusion of an additional turnover compartment as in the case of $PDiam$.

Model selection

The minimum value of the objective function, approximately equal to $-2 \times \log$ -likelihood ($-2LL$), was used to select between candidates during model building through the log-likelihood ratio test (LRT). A decrease of 3.84 or 6.61 in the $-2LL$ —corresponding to a 5% or 1% level of significance, respectively—was considered statistically

significant for nested models differing in one parameter. For comparison across non-nested models, the Akaike information criteria (AIC) was used.¹⁸ In addition to LRT or AIC, precision of parameter estimates expressed as the percentage of relative standard error (RSE[%])—calculated as the ratio (multiplied by 100) between the standard error of the parameter and the corresponding estimate—was also considered, together with the visual inspection of the goodness-of-fit (GOF) plots.

Model evaluation

Once the models for PDiam and movement responses were selected, the evaluation process was performed. Parameter precision was further evaluated by analyzing 500 nonparametric bootstrap data sets using the selected models and calculating the median and the 95% confidence intervals for each of the model parameters. Visual predictive checks (VPCs)¹⁹ corresponding to simulation-based diagnostics were generated to evaluate model performance. A total of 1000 data sets of the same characteristics as the original were simulated using the structure and parameters from the selected models. For each simulated data set and each measurement time, either the 2.5th, 50th, or 97.5th percentiles of the PDiam or the percentage of movement scores of 0, 1, 2, and 3 were calculated. Then the areas covering the 95% prediction intervals of each of the simulated percentiles or each of the movement scores were generated and plotted together with the corresponding raw data.

Data corresponding to the fifth stimulus (the second after surgery) was not used for model development but as an internal validation data set. The model developed for stimuli 1–4 was used to simulate the PDiam and movement grades during the fifth stimulus, and this simulation confronted with the observations. In addition, in the case of pupil, individual model parameters were used to predict the PDiam during the fifth stimulus. Prediction errors (PE)—calculated with Equation (8)—were computed to quantify the precision of the individual predictions for the fifth stimulus and compared with the PE for the previous stimuli.

$$PE_i = 100 \times \sum_{j=1}^n \frac{\text{Pred}_j - \text{Obs}_j}{\text{Obs}_j} \quad (8)$$

where Pred_j and Obs_j , refer to the i th individual model predictions and observations obtained at time j th, respectively.

Software and tools

R Version 3.6.1²⁰ with RStudio²¹ interface (Version 1.2.5001) were used for building the NONMEM data set

TABLE 1 Patient characteristics

| | |
|---|------------------|
| Patients, n | 78 |
| Female, n | 78 |
| Age, years, median (range) | 45 (27–85) |
| Height, cm, median (range) | 160 (140–173) |
| Weight, kg, median (range) | 64 (38–93) |
| Lean body mass, kg, median (range) | 44 (31–58) |
| Body surface area, m^2 , median (range) | 1.65 (1.26–2.04) |

and generating the graphical output. GOF plots were generated with the R packages Xpose²² and ggplot2.²³ VPCs, covariate evaluation, and bootstrap simulations were performed with Perl-Speaks-NONMEM.^{24,25}

RESULTS

Demographic characteristics of the patients included in the study are shown in Table 1. Supplementary material (SM) 1-Figure 1 shows the distribution of the different combinations of propofol and remifentanyl targeted during the study.

Model development

Pupillary reflex dilation

A model considering that the dynamics of the PRD are influenced by the time course of N_{act} provided better fits compared with just one turnover compartment ($\Delta\text{-2LL} = -890$; $p < 0.01$). In Figure 2a, the schematic representation of two compartments required to properly describe the PDiam observations is shown.

Remifentanyl showed significant ($p < 0.01$) effects in (i) reducing of the nociception activation triggered by the application of the electric stimulus and (ii) increasing the first-order rate constant K_D , as represented in Equation (9):

$$\frac{dN_{\text{act}}}{dt} = K_S \times \left(1 + \theta_{\text{ES}} \times \text{ES} \times \frac{1}{1 + \frac{C_{p,\text{remi}}}{C_{50}}} \right) - K_D \times (1 + \theta_{\text{remi}} \times C_{e,\text{remi}}) \times N_{\text{act}} \quad (9)$$

where ES is a variable with a value of 1 during the application of the electrical stimulus and 0 otherwise. θ_{ES} is the parameter accounting for the nociceptive effects of the ES, and C_{50} is the concentration of remifentanyl ($C_{p,\text{remi}}$) reducing the impact of θ_{ES} to half its maximum value. These terms account for the induction of the PRD response by the electrical stimulation and the attenuation by remifentanyl. The term θ_{remi} refers to the slope at which the concentrations of remifentanyl in the

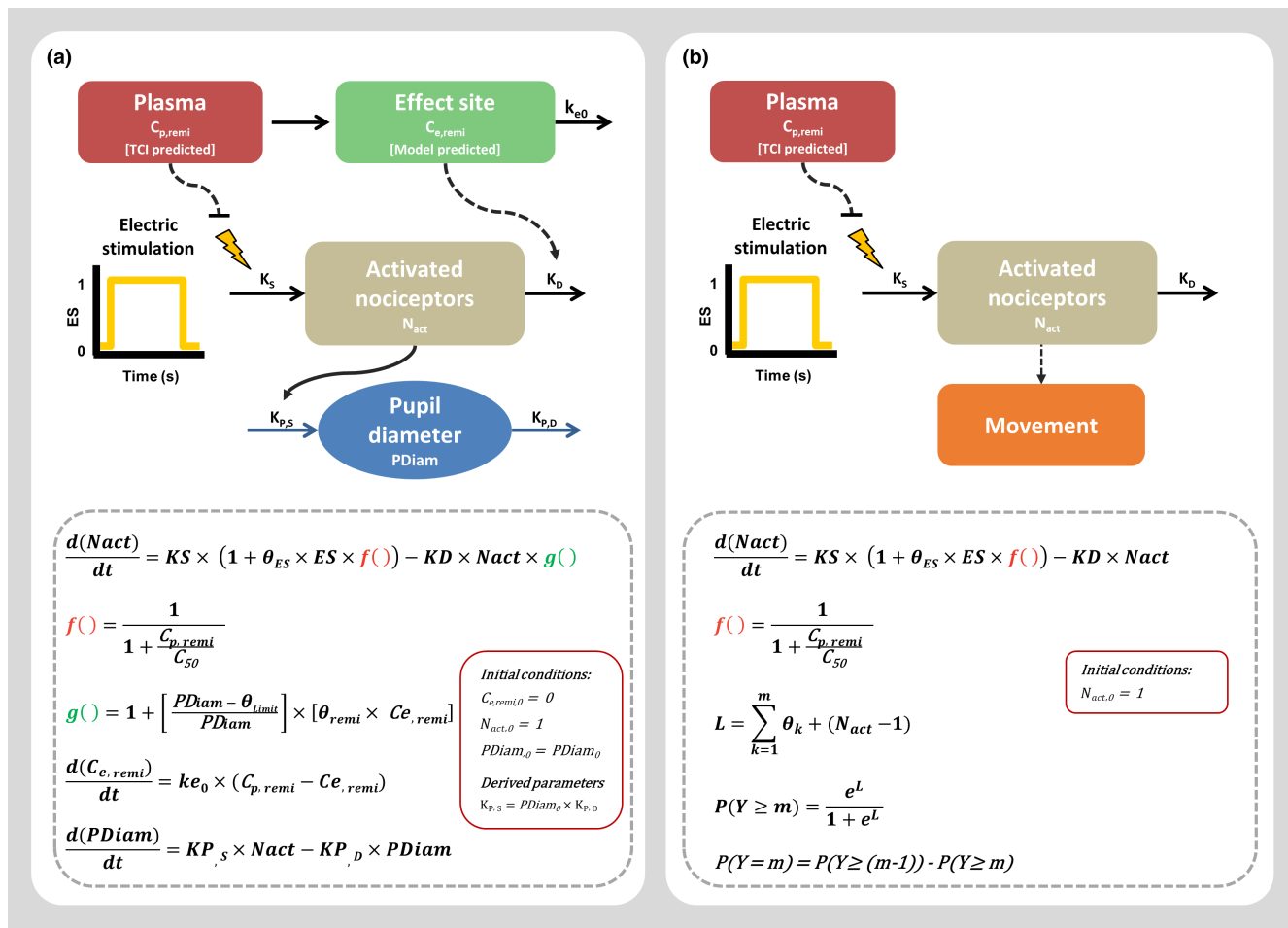


FIGURE 2 Schematic and mathematical representation of the pharmacokinetic/pharmacodynamics models developed for pupil diameter (a) and movement response (b). All parameters are described in the text. Note that in our model, K_s and K_D are the same parameter

effect site increases K_D and is related to the decrease of PDiam over time after administration of remifentanyl. To prevent that remifentanyl could decrease PDiam below physiological constraints, the term $(PDiam - \theta_{Limit})/PDiam$ was incorporated into this effect. Finally, the contribution of propofol was analyzed and did not significantly modified the different processes reflected in the model ($p > 0.05$) (SM 1-Figure 2). Figure 2a shows both the schematic and the full mathematical representation of the structural part of the population model for PDiam.

The model parameters, shown in Table 2, were estimated with good precision. The estimated PDiam at baseline was 3.8 mm. The estimates of the first-order rate constants K_D , $K_{P,D}$, and k_{e0} corresponds to half-lives of 9.5 s, 1.3 s, and 3.56 min, respectively, indicating faster turnovers of N_{act} and PDiam than distribution of remifentanyl from plasma to the effect site. The steady-state concentration of remifentanyl to reduce by half the impact of θ_{ES} and double K_D are 1.15 and 0.67 ng/ml, respectively.

Data supported the estimation of moderate IIV on $PDiam_0$, θ_{ES} , $K_{P,D}$, and θ_{remi} ranging from 24% to 56% coefficient of variation. A correlation of -0.51 was found between random effects associated with $PDiam_0$ and θ_{ES} . As

no tendencies were detected between individual estimates of model parameters and patient characteristics, no further investigation of potential covariate effects was undertaken. Despite that including autocorrelation in the residual model decreased the $-2LL$, the model performed worse as reflected by the individual predictions and VPCs, and therefore autocorrelation was not included in the selected model.

Figure 3 shows the GOF plots (a) and the results of the simulation-based diagnostics (b) corresponding to all data used for model development, both indicating adequate model performance and an absence of model misspecifications. Similar results were found during internal validation using the data corresponding to the fifth stimulus, which are shown in SM 1-Figure 3. SM 2 shows the NMTRAN code corresponding to the selected model.

Reflex movement

In the movement response, the addition of the second turnover compartment did not improve the fit significantly ($p > 0.05$). Remifentanyl elicited a significant effect

TABLE 2 Model parameter estimates

| Parameter | Estimate | RSE (%) | 2.5th–97.5th | Shrinkage, % |
|--|----------|---------|------------------------------|--------------|
| Pupillary reflex dilation response | | | | |
| K_S (s^{-1}) | 0.0726 | 19.6 | 0.0203–0.152 | – |
| PDiam ₀ (mm) | 3.80 | 3.3 | 3.57–4.02 | – |
| IIV PDiam ₀ (%) | 24.6 | 7.7 | 20.9–28.4 | 1 |
| $K_{P,D}$ (s^{-1}) | 0.531 | 13.9 | 0.294–1.07 | – |
| IIV $K_{P,D}$ (%) | 54.4 | 22.0 | 31.5–107 | 26 |
| θ_{ES} | 1.54 | 11.0 | 1.10–4.33 | – |
| IIV θ_{ES} (%) | 49.6 | 11.5 | 36.9–63.7 | 9 |
| Cov ($\omega^2_{PDiam_0}, \omega^2_{\theta_{ES}}$) | –0.0574 | 18.7 | –0.0978 to –0.0236 | – |
| C_{50} (ng/ml) | 1.15 | 14.0 | 0.868–1.52 | – |
| θ_{remi} (ml/ng) | 1.50 | 12.9 | 1.10–2.39 | – |
| IIV θ_{remi} (%) | 55.6 | 8.7 | 44.1–73.9 | 2 |
| k_{e0} (s^{-1}) | 0.00324 | 8.0 | $(2.67–3.82) \times 10^{-3}$ | – |
| θ_{Limit} (mm) | 1.41 | 6.1 | 1.18–1.61 | – |
| Residual error (%) | 9.90 | 6.6 | 8.50–11.0 | 3 |
| Movement response | | | | |
| K_S (s^{-1}) | 0.437 | 13.9 | 0.336–0.617 | – |
| θ_{ES} | 6.63 | 8.2 | 5.67–7.98 | – |
| θ_1 | –4.90 | 4.0 | –5.38––4.58 | – |
| θ_2 | –0.754 | 11.2 | –0.916––0.584 | – |
| θ_3 | –0.978 | 17.1 | –1.32––0.697 | – |
| $\theta_{1,1}$ | 1.76 | 13.1 | 1.30–2.17 | – |
| $\theta_{2,2}$ | 1.93 | 16.2 | 1.31–2.63 | – |
| $\theta_{3,3}$ | 2.43 | 16.7 | 1.58–3.50 | – |
| C_{50} (ng/ml) | 0.617 | 23.3 | 0.360–1.02 | – |

Notes: IIV is expressed as percentage coefficient of variation calculated as $\sqrt{\omega^2 - 1} \times 100$, where ω^2 corresponds to the variance of the random effects. The rest of the terms are defined in the main text.

Abbreviations: Cov, covariance; RSE(%), percentage of relative standard error.

($p < 0.01$), reducing the nociceptive effects triggered by electric stimulation as it was previously described for PDiam. Figure 2b shows the schematic and mathematical representation of the model for movement reflex. Regarding the structure of the logit, the function $h()$ (see Equation 6) has as argument $N_{act} - 1$, which gives the value of zero in unperturbed conditions. The addition of a random effect on the L was not significant ($p > 0.05$), and as in the case of the PDiam, propofol was not shown to significantly contribute to antinociception.

The possibility that the probability of each score at a certain time is influenced at least in part on the score achieved in the previous time (first-order Markov process) was also investigated. Addition of the parameters accounting for all transitions resulted in a significant ($p < 0.01$) improvement in the predictions, particularly for movement Grades 1 and 3 (SM 1-Figure 4, Panel c).

Table 2 also lists the model parameter estimates corresponding to the movement response. All parameters were estimated precisely as confirmed by the low RSE and 95%

confidence intervals. The estimate of K_D corresponds to a value of half-life of 1.58 s, and C_{50} is estimated as 0.617 ng/ml. In absence of stimulus, the probability of transitioning to movement is negligible ($<0.8\%$). Once a certain grade is reached, the probability of maintaining the movement intensity is 85%, 87%, and 92% for Grades 1, 2, and 3 and returning probabilities to baseline are 15%, 13%, and 8%, respectively.

Results shown in Figure 4, corresponding to GOF (left) and VPCs pooling all data together (right), indicate that the model described the data properly. SM 3 shows the NMTRAN code corresponding to the selected model incorporating the Markov elements.

SM 1-Figure 5 splits the VPC per stimulus and shows, in addition, good model performance for the movement responses gathered in stimulus 5, which were used for internal validation purposes. Our model was also able to capture the number of transitions between movement grades observed in the study: 261 for the raw data and a median of 272 for the model predictions (248 to 297, 95% confidence interval).

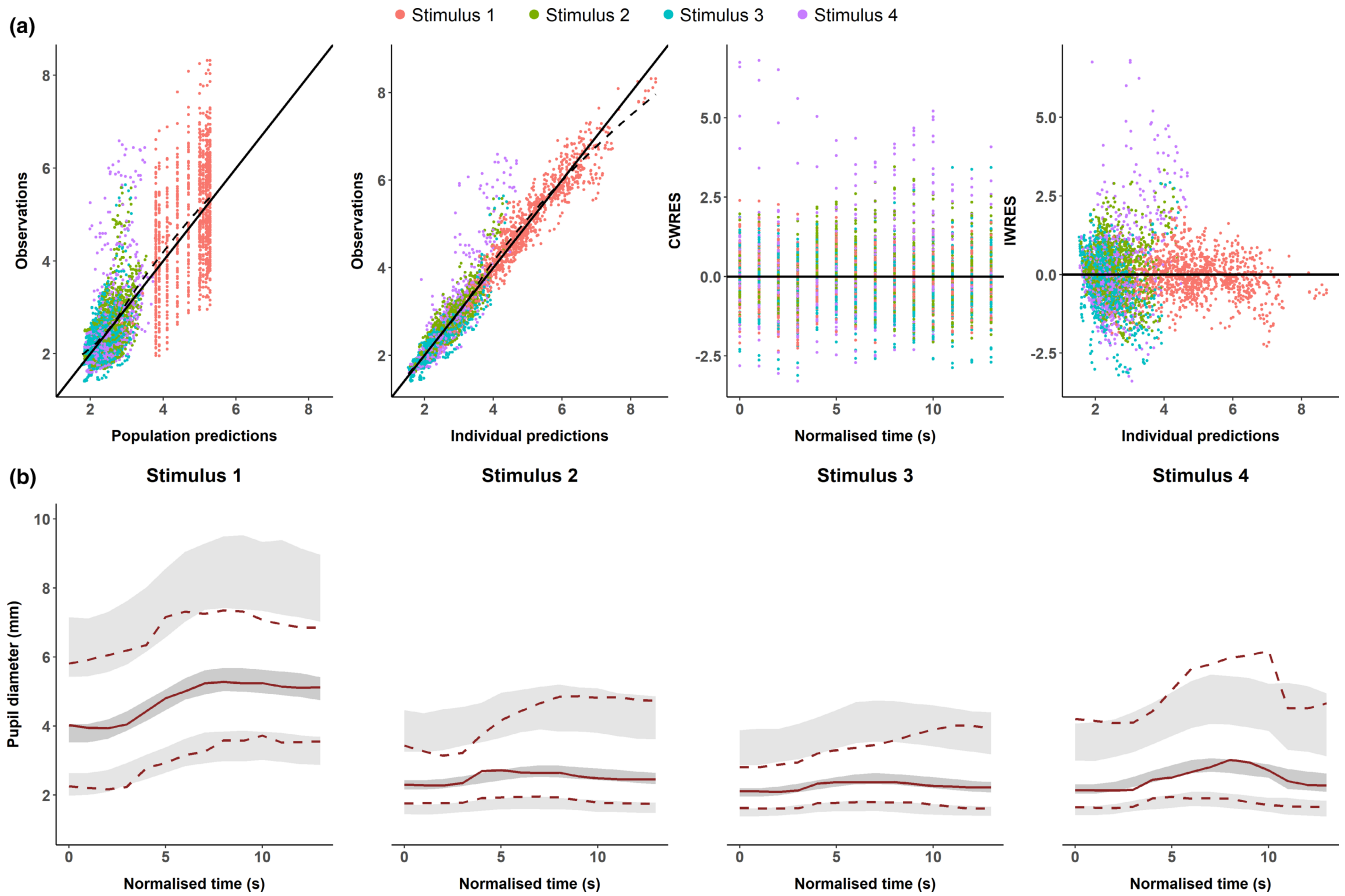


FIGURE 3 Pupil diameter model evaluation. (a) Goodness-of-fit plots. Data are colored according to the stimulus: 1, red; 2, green; 3, blue; 4, purple. Dashed line represents the loess smoothing curve. (b) Visual predictive checks for Stimulus 1 to Stimulus 4. Median (solid line) and 2.5th and 97.5th percentiles (dashed lines) of observed data compared with 95% prediction intervals (shaded area) for the median and 2.5th and 97.5th percentiles based on 1000 simulations. CWRES, conditional weighted residuals; IWRES, individual weighted residuals

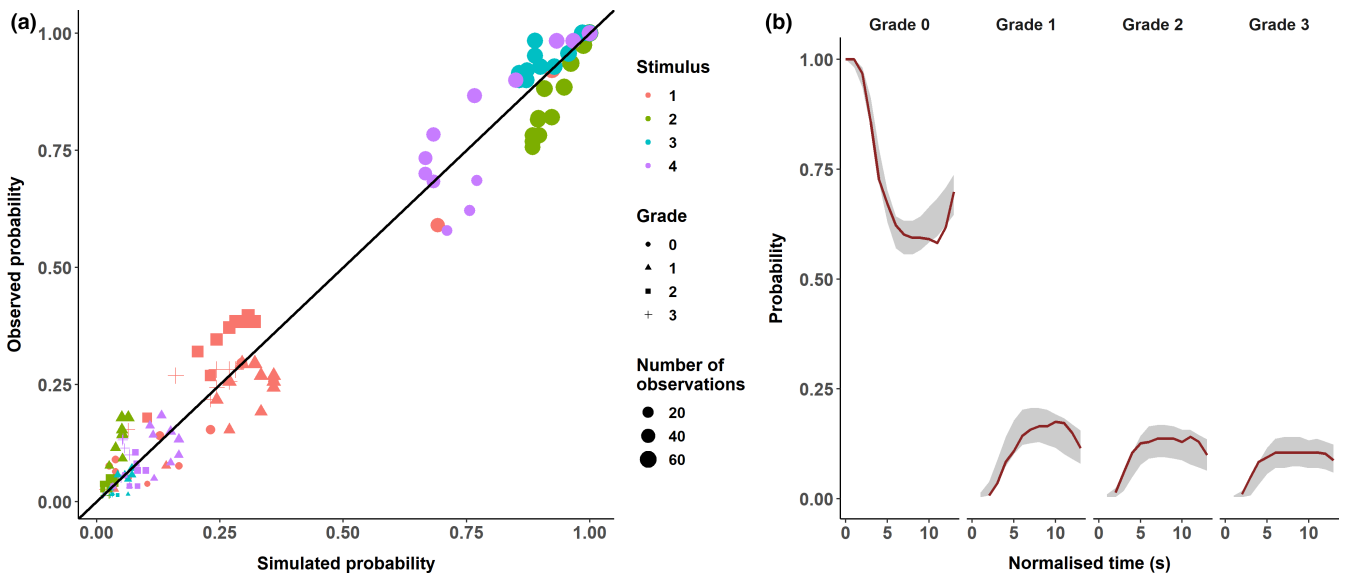


FIGURE 4 Movement response model evaluation. (a) Observed versus predicted probability of movement for each grade and number of stimulus calculated from 500 simulations. Solid line is the identity representing perfect fit. (b) Visual predictive checks stratified by grade. Solid line corresponds to the median probability calculated from raw data, and the shaded areas represented the 95% prediction intervals computed from 1000 simulations

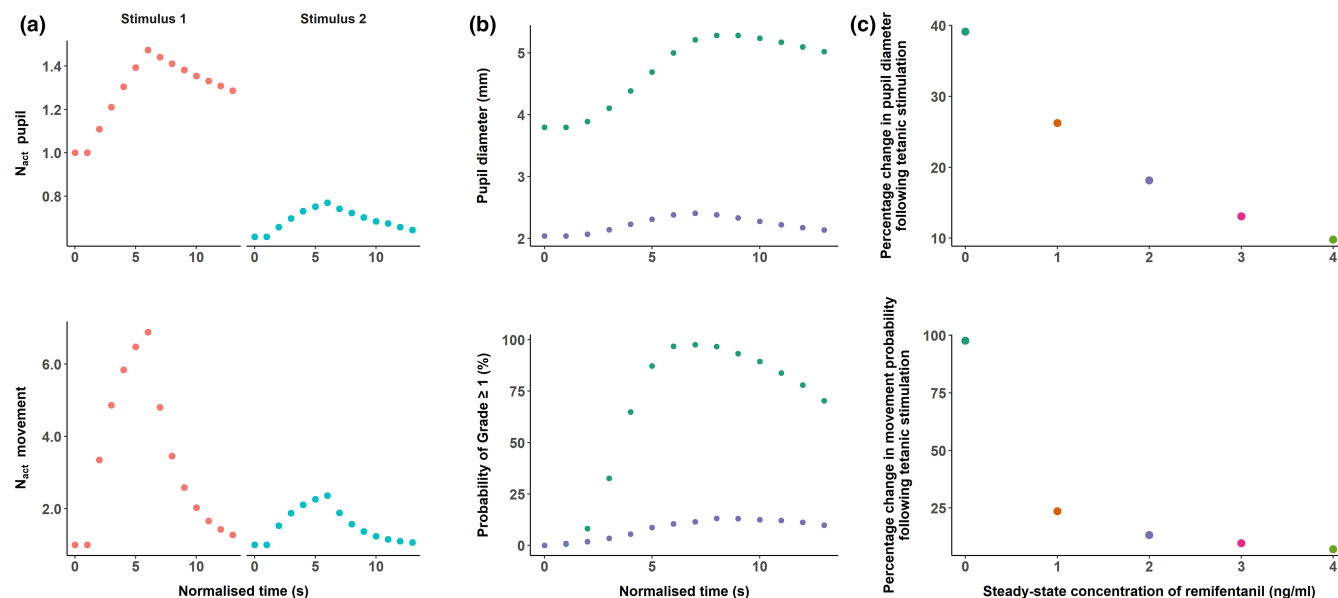


FIGURE 5 Models exploration. (a) Dynamics of nociceptor activation. (b) Pupil diameter and probability of movement in response to tetanic stimulation in absence (blue) or presence of remifentanyl at 2 ng/ml steady-state concentration (purple). (c) Percentage change in pupil diameter and probability of movement after tetanic stimulation at different steady-state concentrations of remifentanyl

Model exploration

SM 1-Figure 4 explores the impact of some of the key components of the selected models on the measured responses. Panels A and B show the changes in pupil response after the administration of remifentanyl and graphically explores the individual contribution of the model effects to these changes. Figure 5a shows the time course of the predicted degree of nociceptor activation for movement and PRD, and despite similar trends, movement appears to be associated to a faster turnover. The relationship between the amplitude in the pupil response profile and the probability of movement versus steady-state remifentanyl concentrations are shown in Figure 5b,c. Similar patterns between the two variables can be observed again, with the degree of steepness higher for movement.

Clinical applicability

Model-based simulations were performed to identify the concentration of remifentanyl at which 80% of patients would not experience movement after the delivery of a tetanic current ranging from 1.2 to 0.8 times the one used in the experimental procedure (60 mA). The simulation assumed an intensity of 1.2 for laryngoscopy and intubation while an intensity of 0.8 was assumed to represent a less painful surgical wound closure. For this purpose, we simulated 1000 individuals receiving electric stimulus of varying intensity at steady-state concentrations of remifentanyl from 0 to 4 ng/ml and computed the

percentage of individuals not experiencing movement. A steady-state concentration of 2 ng/ml was found to inhibit movement in 81% percent of the individuals with the experimental stimulus intensity and 77.8% and 83.1% of the individuals with a 20% increase and reduction in the stimulus intensity, respectively.

This concentration (2 ng/ml steady state) was subsequently used to simulate the PDiam of 1000 individuals from baseline to the end of a PRD. PDiam before electric stimulation for 80% of the individuals ranged from 1.69 to 2.61 mm (10th and 90th percentiles) and were distinctly different from the PDiam at baseline (2.71 and 5.25 mm, 10th and 90th percentiles, respectively) due to the pharmacologic effects of remifentanyl. However, no correlation could be established between PRD and the prestimulus or basal (PDiam₀) pupil, thus preventing recommendations on treatment individualization based on pre-stimulus pupil size.

DISCUSSION

We have described both the PRD and reflex movement responses to noxious stimulation using a semimechanistic population pharmacokinetic/pharmacodynamics model to investigate similarities between the underlying mechanisms governing these two responses and the effects of remifentanyl. Using this approach, we demonstrated that movement and PRD are equally depressed following remifentanyl infusions. These data suggest that pupilary dilation and movement are initiated from a common source which is depressed by opioids.

The afferent noxious stimulus activates several sites within the pain matrix that in turn directly or indirectly inhibits the Edinger–Westphal nucleus and dilate the pupil. The RVM, gigantocellular reticular nucleus, and the locus coeruleus are possible sources of this inhibition.^{26,27}

These same nuclei have descending projections into the spinal cord that influence the withdrawal reflex. “Off-cells” in the RVM for example are antinociceptive and are inhibited by noxious stimuli.^{28,29} This inhibition of “off-cells” is blocked by opioids. We hypothesize that the RVM and the EW nucleus are affected by nociception and opioids in a similar manner. Which after further investigation and confirmatory studies, could thereby allow the anesthesia provider to observe PRD as a measure of opioid effect on suppression of movement.

The final models selected in the current investigation have been carefully and extensively evaluated using both GOF plots and simulation-based diagnostics while being validated internally with a set of data not used during model building. Data were accurately described, and all parameters were estimated with good precision. The models were capable of handling data gathered under different experimental conditions such as (i) the absence or presence of the analgesic drug and (ii) before and after surgery, indicating model robustness to support the conclusions of this work.

The use of changes in pupillary parameters as a surrogate marker of analgesic effects has received considerable attention in the past. PRD was shown to be useful to assess the nociception/antinociception balance and titrate opioid administration³⁰ as PRD is triggered by noxious stimuli during general anesthesia^{6,7} and diminished by opioid administration.⁸ Our results support the observations by Barvais et al.⁸ for the correlation between remifentanyl Ce and percentage PRD as shown in [Figure 5](#).

Pharmacokinetic/pharmacodynamics modeling has been previously done for the pupillary light reflex, demonstrating the effects of opioid drugs,^{31–35} and to a lesser extent, drugs modulating noradrenergic pathways.^{36–38} However, there are no previous modeling studies for PRD and how nociception and opioids influence it. Although only using isolated PDiam measurements, instead of the light reflex, Skarke et al.³⁹ modeled independently pupil and pain tolerance in response to electric pain stimulation and showed that (i) the effect site equilibration half-life ($t_{1/2_ke0}$) obtained for pupil was almost identical to the one from pain tolerance data and (ii) changes in both variables occur in parallel. Recently, Mangas-Sanjuan et al.⁴⁰ modeled the PDiam effects of the active components of axamadol and found that pupillary changes correlated linearly with the area under the curve of the cold pressor test.

Pharmacodynamics of remifentanyl is represented by values of C_{50} ranging from 0.92 to 11.2 ng/ml for other

indicators of central activity such as arterial pressure,^{41,42} spectral edge frequency of the electroencephalogram,¹⁴ and respiratory depression.^{43,44} Remarkably, the corresponding estimates obtained in the current evaluation are in the same order of magnitude as those reported previously. Onset of action of remifentanyl is fast with values of $t_{1/2_ke0}$ of 0.53 to 2.48 min.^{14,41–44} The value of $t_{1/2_ke0}$ found in this study is 3.5 min; however, for the additional effect of K_D , the model considers an instantaneous equilibrium between the central and the effect site compartment. Those discrepancy might be caused by the fact that we predicted¹⁴ but did not measure plasma concentrations. Alternatively, it might well be that the region in the central nervous system in which remifentanyl elicits analgesia is, at least from a distribution point of view, different from those contributing to cortical effects and respiratory depression.⁴⁴

This study has the objective to evaluate whether PDiam and movement responses ensue from a nociceptive stimulus and if the counteraction of remifentanyl shares a common underlying pathway. In this context, one important aspect that deserves consideration is the granularity at which we measured the responses. The PRD was measured 67 times per second and the movement response each second during and after electrical stimulation in several occasions, resulting in an appropriate experimental framework to achieve our objective. This is the first pharmacodynamic model focusing on the pupillary effect of opioids ever to use this time resolution.

There are several possibilities to analyze the current data, for instance a simultaneous analysis where an unobserved variable (i.e., N_{act}) is scaled differently for each of the two clinical end points. We decided to use an unbiased approach consisting on modeling the two end points independently hypothesizing a common core mechanism (the turnover model for N_{act}) triggering a reflex movement response. The results from our analysis suggest that PRD and movement responses do share that mechanism as the model parameters are essentially similar for the turnover rates and remifentanyl related effect parameters. However, the fact that both variables were not modeled simultaneously represents a limitation. The model indicates that differences between both responses appear up-stream because the incorporation for PDiam of an additional turnover compartment, and for movement response of the Markov element contributing to maintain nociception, provided similar temporal patterns (see [Figure 5b](#)). Markov elements have been commonly identified in the analysis of noncontinuous responses (count or ordered as well as nonordered categorical) and in this evaluation contributed to improve the description of the data.^{45,46}

This is an innovative model that attempts to simultaneously describe the antinociceptive effect of remifentanyl in

the transduction and transmission component using the plasma concentration and the modulation phase through the effect site concentrations while describing how both influence PRD and movement in response to a noxious stimulus.

The knowledge provided by this investigation may allow a better understanding of the underlying phenomenon of nociception/antinociception during general anesthesia and allow for rational opioid dosing to prevent the central nervous system activation that would elicit a movement response and use the PRD as a surrogate reliable measure of adequate antinociception in the clinical setting.

ACKNOWLEDGEMENTS

A. Chen was supported by a J. William Fulbright Foreign Scholarship 2019–2020.

CONFLICT OF INTEREST

II-A is currently employed by AstraZeneca. CG and EWJ are employees of Quantum Medical. PLG has received honoraria from Quantum Medical. All other authors declared no competing interests for this work.

AUTHOR CONTRIBUTIONS

All authors wrote the manuscript. PLG and MDL designed the research. SV, MA, SJ, and PLG performed the research. NMA, II-A, and IFT analyzed the data. AC, AP, CG, EWJ, PC-M, and JFV contributed new reagents/analytical tools.

REFERENCES

- Rantanen M, Yppärilä-Wolters H, van Gils M, et al. Tetanic stimulus of ulnar nerve as a predictor of heart rate response to skin incision in propofol-remifentanyl anaesthesia. *Br J Anaesth*. 2007;99:509–513.
- Schlereth T, Birklein F. The sympathetic nervous system and pain. *NeuroMolecular Med*. 2008;10:141–147.
- Holte K, Kehlet H. Postoperative ileus: a preventable event. *Br J Surg*. 2000;87:1480–1493.
- Larson MD, Behrends M. Portable infrared pupillometry. *Anesth Analg*. 2015;120:1242–1253.
- Larson MD, Sessler DI. Pupillometry to guide postoperative analgesia. *Anesthesiology*. 2012;116:980–982.
- Larson M, Kurz A, Sessler D, Dechert M, Bjorksten A, Tayefeh F. Alfentanil blocks reflex pupillary dilation in response to noxious stimulation but does not diminish the light reflex. *Anesthesiology*. 1997;87:849–855.
- Larson MD, Sessler DI, Washington DE, Merrifield BR, Hynson JA, McGuire J. Pupillary response to noxious stimulation during isoflurane and propofol anesthesia. *Anesth Analg*. 1993;76:1072–1078.
- Barvais L, Engelman E, Eba JM, Coussaert E, Cantraine F, Kenny GN. Effect site concentrations of remifentanyl and pupil response to noxious stimulation. *Br J Anaesth*. 2003;91:347–352.
- Ossipov MH, Dussor GO, Porreca F. Central modulation of pain. *J Clin Invest*. 2010;120:3779–3787.
- Fields H. State-dependent opioid control of pain. *Nat Rev Neurosci*. 2004;5:565–575.
- Larson MD, Berry PD. Supraspinal pupillary effects of intravenous and epidural fentanyl during isoflurane anesthesia. *Reg Anesth Pain Med*. 2000;25:60–66.
- Schnider TW, Minto CF, Shafer SL, et al. The influence of age on propofol pharmacodynamics. *Anesthesiology*. 1999;90:1502–1516.
- Schnider T, Minto C, Gambus P, et al. The influence of method of administration and covariates on the pharmacokinetics of propofol in adult volunteers. *Anesthesiology*. 1998;88:1170–1182.
- Minto C, Schnider T, Egan T, et al. Influence of age and gender on the pharmacokinetics and pharmacodynamics of remifentanyl I. Model Development. *Anesthesiology*. 1997;86:10–23.
- Beal SL, Sheiner LB, Boeckmann AJ, Bauer RJ. NONMEM 7.4. 3 Users Guides (1989–2018). Hanover, MD, USA ICON Dev. Solut. (2018).
- Karlsson MO, Beal SL, Sheiner LB. Three new residual error models for population PK/PD analyses. *J Pharmacokinetic Biopharm*. 1995;23:651–672.
- Dayneka NL, Garg V, Jusko WJ. Comparison of four basic models of indirect pharmacodynamic responses. *J Pharmacokinetic Biopharm*. 1993;21:457–478.
- Ludden TM, Beal SL, Sheiner LB. Comparison of the Akaike Information Criterion, the Schwarz criterion and the F test as guides to model selection. *J Pharmacokinetic Biopharm*. 1994;22:431–445.
- Holford N. The visual predictive check—superiority to standard diagnostic (Rorschach) plots. PAGE 14 (2005) Abstr 738 [www.page-meeting.org/?abstract=738]. Accessed April 1, 2020.
- R Core Team (2020). R: A language and environment for statistical computing. R Foundation for Statistical Computing. URL <https://www.R-project.org/>. Accessed July 7, 2019.
- RStudio Team (2019). RStudio: Integrated Development for R. RStudio, Inc., URL <http://www.rstudio.com/>. Accessed July 7, 2019.
- Jonsson EN, Karlsson MO. Xpose - an S-PLUS based population pharmacokinetic/pharmacodynamic model building aid for NONMEM. *Comput Methods Programs Biomed*. 1998;58:51–64.
- Wickham H. *ggplot2: Elegant Graphics for Data Analysis*. Springer-Verlag; 2016.
- Lindbom L, Ribbing J, Jonsson EN. Perl-speaks-NONMEM (PsN) - a Perl module for NONMEM related programming. *Comput Methods Programs Biomed*. 2004;75:85–94.
- Lindbom L, Pihlgren P, Jonsson N. PsN-Toolkit - a collection of computer intensive statistical methods for non-linear mixed effect modeling using NONMEM. *Comput Methods Programs Biomed*. 2005;79:241–257.
- Joshi S, Li Y, Kalwani RM, Gold JJ. Relationships between pupil diameter and neuronal activity in the locus coeruleus, colliculi, and cingulate cortex. *Neuron*. 2016;89:221–234.
- Jinks SL, Bravo M, Satter O, Chan Y-M. Brainstem regions affecting minimum alveolar concentration and movement pattern during isoflurane anesthesia. *Anesthesiology*. 2010;112:316–324.
- Fields HL, Heinricher MM. Brainstem modulation of nociceptor-driven withdrawal reflexes. *Ann N Y Acad Sci*. 1989;563:34–44.
- Fields HL, Heinricher MM, Mason P. Neurotransmitters in nociceptive modulatory circuits. *Annu Rev Neurosci*. 1991;14:219–245.
- Vide S, Castro A, Antunes P, et al. Pharmacodynamic modeling of the effect of remifentanyl using the Pupillary Pain Index. *J Clin Monit Comput*. 2020;34:319–324.

31. Westerling D, Persson C, Høglund P. Plasma concentrations of morphine, morphine-3-glucuronide, and morphine-6-glucuronide after intravenous and oral administration to healthy volunteers: Relationship to nonanalgesic actions. *Ther Drug Monit.* 1995;17:287–301.
32. Dershwitz M, Walsh JL, Morishige RJ, et al. Pharmacokinetics and pharmacodynamics of inhaled versus intravenous morphine in healthy volunteers. *Anesthesiology.* 2000;93:619–628.
33. Lötsch J, Skarke C, Schmidt H, Grösch S, Geisslinger G. The transfer half-life of morphine-6-glucuronide from plasma to effect site assessed by pupil size measurement in healthy volunteers. *Anesthesiology.* 2001;95:1329–1338.
34. Schmidt H, Lötsch J. Pharmacokinetic-pharmacodynamic modeling of the miotic effects of dihydrocodeine in humans. *Eur J Clin Pharmacol.* 2007;63:1045–1054.
35. Ladebo L, Foster DJR, Abuhelwa AY, et al. Population pharmacokinetic-pharmacodynamic modelling of liquid and controlled-release formulations of oxycodone in healthy volunteers. *Basic Clin Pharmacol Toxicol.* 2020;126:263–276.
36. Valles J, Obach R, Menargues A, Pruñonosa J, Jane F. A Pharmacokinetic-pharmacodynamic linking model for the α 2-adrenergic antagonism of idazoxan on clonidine-induced mydriasis in the rat. *J Pharm Pharmacol.* 1995;47:157–161.
37. Lindauer A, Siepmann T, Oertel R, et al. Pharmacokinetic/pharmacodynamic modelling of venlafaxine: Pupillary light reflex as a test system for noradrenergic effects. *Clin Pharmacokinet.* 2008;47:721–731.
38. Liem-Moolenaar M, de Boer P, Timmers M, et al. Pharmacokinetic-pharmacodynamic relationships of central nervous system effects of scopolamine in healthy subjects. *Br J Clin Pharmacol.* 2011;71:886–898.
39. Skarke C, Darimont J, Schmidt H, Geisslinger G, Lötsch J. Analgesic effects of morphine and morphine-6-glucuronide in a transcutaneous electrical pain model in healthy volunteers. *Clin Pharmacol Ther.* 2003;73:107–121.
40. Mangas-Sanjuan V, Pastor JM, Rengelshausen J, Bursi R, Troconiz IF. Population pharmacokinetic/pharmacodynamic modelling of the effects of axomadol and its O-demethyl metabolite on pupil diameter and nociception in healthy subjects. *Br J Clin Pharmacol.* 2016;82:92–107.
41. Glass PSA, Hardman D, Kamiyama Y, et al. Preliminary pharmacokinetics and pharmacodynamics of an ultra-short-acting opioid: Remifentanyl (GI87084B). *Anesth Analg.* 1993;77:1031–1040.
42. Hannam JA, Borrat X, Troconiz IF, et al. Modeling respiratory depression induced by remifentanyl and propofol during sedation and analgesia using a continuous noninvasive measurement of pCO₂. *J Pharmacol Exp Ther.* 2016;356:563–573.
43. Bouillon T, Bruhn J, Radu-Radulescu L, Andresen C, Cohane C, Shafer SL. A model of the ventilatory depressant potency of remifentanyl in the non-steady state. *Anesthesiology.* 2003;99:779–787.
44. Olofson E, Boom M, Nieuwenhuijs D, et al. Modeling the non-steady state respiratory effects of remifentanyl in awake and propofol-sedated healthy volunteers. *Anesthesiology.* 2010;112:1382–1395.
45. Karlsson M. A pharmacodynamic Markov mixed-effect model for the effect of temazepam on sleep. *Clin Pharmacol Ther.* 2000;68:175–188.
46. Trocóniz IF, Plan EL, Miller R, Karlsson MO. Modelling overdispersion and markovian features in count data. *J Pharmacokinetic Pharmacodyn.* 2009;36:461–477.
47. SMART Servier Medical Art. <https://smart.servier.com/>. Accessed May 31, 2021.
48. Freepik. <https://www.freepik.com/>. Accessed June 6, 2021.

SUPPORTING INFORMATION

Additional supporting information may be found in the online version of the article at the publisher's website.

How to cite this article: Marco-Ariño N, Vide S, Agustí M, et al. Semimechanistic models to relate noxious stimulation, movement, and pupillary dilation responses in the presence of opioids. *CPT Pharmacometrics Syst Pharmacol.* 2022;11:581–593. doi:[10.1002/psp4.12729](https://doi.org/10.1002/psp4.12729)